Materials Letters 161 (2015) 168–171

Contents lists available at ScienceDirect

Materials Letters

journal homepage: www.elsevier.com/locate/matlet

Epitaxially strained $BaTiO_3$ thin films on $LaAlO_3$ substrates with $La_{0.5}Sr_{0.5}MnO_3$ electrodes: Enhanced ferroelectric property and domain structure

Yoonho Ahn [a,*], Jeongdae Seo [a], Joonkyung Jang [b], Jong Yeog Son [a,*]

[a] Department of Applied Physics and Institute of Natural Sciences, College of Applied Science, Kyung Hee University, Yongin 446-701, South Korea
[b] Department of Nanoenergy Engineering, Pusan National University, Busan 609-735, South Korea

ARTICLE INFO

Article history:
Received 12 May 2015
Received in revised form
25 June 2015
Accepted 16 August 2015
Available online 18 August 2015

Keywords:
Thin film
$BaTiO_3$
Ferroelectric polarization
Domain
Domain wall energy

ABSTRACT

$BaTiO_3$ (BTO) thin films were epitaxially deposited on $LaAlO_3$(LAO) substrates with epitaxial $La_{0.5}Sr_{0.5}MnO_3$(LSMO) electrodes by pulsed laser deposition. We confirmed that the epitaxial BTO thin films on LSMO/LAO substrates remarkably showed the increased remnant polarization in comparison with the epitaxial BTO thin films on Pt/MgO substrates. It was inferred that the enhanced ferroelectric polarization in the epitaxial BTO thin films on LSMO/LAO substrates arose from the increased tetragonality with the *c*/*a* ratio of 1.04. Piezoresponse force microscopy study revealed that the epitaxial BTO thin film on LSMO/LAO substrate possessed higher domain wall energy than that of the $PbTiO_3$ thin films, which implies fine domain structure of the epitaxial BTO thin films on LSMO/LAO substrates.

1. Introduction

Ferroelectric thin films have been widely investigated for various applications such as non-volatile random access memories (NVRAMs), piezoelectric power generators, solar cells, and photovoltaic devices [1–4]. The most well known ferroelectric thin films are lead zirconate titanate (PZT) systems because of their high ferroelectric polarizations and piezoelectric coefficients. However, the toxicity of the PZT systems is the critical problem we are facing at the moment. To replace PZT thin films, a variety of lead-free ferroelectric thin films have been developed. In particular, $BaTiO_3$ (BTO) thin films have widely attracting attention as ferroelectric oxides with ABO_3 perovskite structure. Compared to $BiFeO_3$ (BFO) thin films, BTO thin films have shown relatively good physical properties such as high dielectric constant, low dielectric loss, and low leakage current [5–7].

Meanwhile, most lead-free ferroelectric thin films have not shown high remnant polarization, although BFO thin films exhibited values close to PZT thin films [8,9]. Recently many efforts have been made to control and increase physical properties of the lead-free ferroelectric thin films. Substitution at A or B site with transition metals and rare-earth elements have made it possible to enhance ferroelectric properties, which can be explained by distortion of the crystal structure result from the substitution [10–12]. For example, the Mn or La substituted BTO thin films exhibited the enhanced ferroelectric property [13,14]. In another case, the strained thin films fabricated by using the lattice misfit between thin films and substrates (buffer layers and bottom electrodes) have also shown the increased remnant polarization [15,16] which is similar to the doping and oxygen vacancy (point defect) effects in ferroelectric thin films. By adopting suitable lattice constants and thermal expansion coefficients between thin films and substrates, the strain can be induced and controlled. In this study, we fabricated epitaxially strained BTO thin films on $LaAlO_3$(LAO) substrates using $La_{0.5}Sr_{0.5}MnO_3$(LSMO) electrodes to enhance ferroelectric properties of BTO thin films. The epitaxially strained BTO thin films exhibited the increased remnant polarization when compared to the epitaxial BTO thin films on Pt/MgO substrates which were previously reported in our work [13]. To estimate the domain wall energy, we observed the ferroelectric domain structure of the epitaxially strained BTO thin films by using piezoresponse force microscopy (PFM).

2. Experimental procedure

Epitaxial BTO thin films were grown on LAO substrates using LSMO bottom electrodes by pulsed laser deposition (PLD) method. The used substrates were (100) oriented LAO, which has a pseudocubic structure with $a=3.79$ Å. The bottom electrodes on LAO

* Corresponding authors.
E-mail addresses: yahn@khu.ac.kr (Y. Ahn), jyson@khu.ac.kr (J.Y. Son).

http://dx.doi.org/10.1016/j.matlet.2015.08.080
0167-577X/

substrates were deposited from stoichiometric LSMO targets commercially available. The targets of BTO pellets for thin film deposition were prepared by conventional solid-state reaction method. A frequency tripled ($\lambda = 355$ nm) Nd:YAG laser with a power of 2×10^4 J/m^2 was used at a frequency of 2 Hz and the distance between the targets and the substrates was 5 cm. The base pressure was about 1.33×10^{-4} Pa, and the substrate temperature was set to 850 °C under an oxygen pressure of 6.65 Pa. The thicknesses of the LSMO electrodes and LAO substrates could be achieved by controlling the number of PLD pulses. After deposition, BTO thin films were cooled down to room temperature in oxygen ambient at 4.0×10^4 Pa. Pt top electrode with 100 μm diameter and thickness of 100 nm on the BTO thin film was fabricated to prepare Pt/BTO/LSMO capacitor using RF magnetron sputtering technique. The electrode was then annealed at 400 °C for 5 min before measuring the ferroelectric polarization using an RT66A (Radiant Technologies, Ins.) test system at 2 kHz. Atomic force microscopy (AFM) and PFM were used to examine their surface morphology and ferroelectric domain structure respectively.

3. Results and discussion

Fig. 1(a) shows a schematic drawing of BTO thin film on LSMO/LAO substrate. To fabricate stained BTO thin films on LAO substrates, we used epitaxially deposited LSMO bottom electrode films. To maximize the strain of the LSMO electrodes under the influence of the LAO substrates, we kept the thickness of LSMO electrode films to be about 15 nm. We measured x-ray diffraction (XRD) patterns of a 100 nm thick BTO thin film on the LSMO/LAO substrate as shown in Fig. 1(b) and (c). Fig. 1(b) shows XRD θ–2θ scan of the BTO thin film, where (001) and (002) peaks are observed without any other peaks along the (00l) direction. The full width at half maximums (FWHMs) of the (001) and (002) peaks were estimated to be about 0.6° and 0.7°, respectively. In a rocking curve experiment, the FWHMs of the (001) and (002) peaks were also measured to be 0.9° and 0.8°, respectively although not shown here. These low FWHMs values indicate that the BTO thin film has a good crystallinity along the out-of-plane. From the (001) and (002) peaks of the BTO thin film, we obtained a c-lattice constant of 4.080 Å which was elongated from its bulk lattice constant of 4.017 Å.

To confirm the in-plane crystallinity of the BTO thin film, we performed the azimuth angle scan of the (101) peaks around the c-axis, namely the (001) peak in the BTO thin film. Fig. 1(c) shows the Φ scan of the (101) BTO and (101) LAO peaks. Four-fold symmetry of all in-plane peaks was observed. The unit cells of the BTO thin film and LAO substrate were positioned in parallel along the in-plane direction. From the relative position of two in-plane peaks, we can infer that the BTO thin film was epitaxially grown on LAO substrate. For the BTO thin film, the FWHM of the (101) rocking curve was measured to be about 0.8°, which indicates the well-defined crystallinity along the in-plane orientation. From the (101) peak of BTO thin film, we could estimate a a-lattice constant of 3.924 Å, which was slightly smaller than its bulk lattice constant of 3.978 Å. The deposited BTO thin film showed relatively high c/a ratio of about 1.04. Based on these data, we can infer that the epitaxially grown BTO thin film is likely to show a good ferroelectric property due to the increased tetragonality.

Fig. 2 shows surface morphology and ferroelectric domain

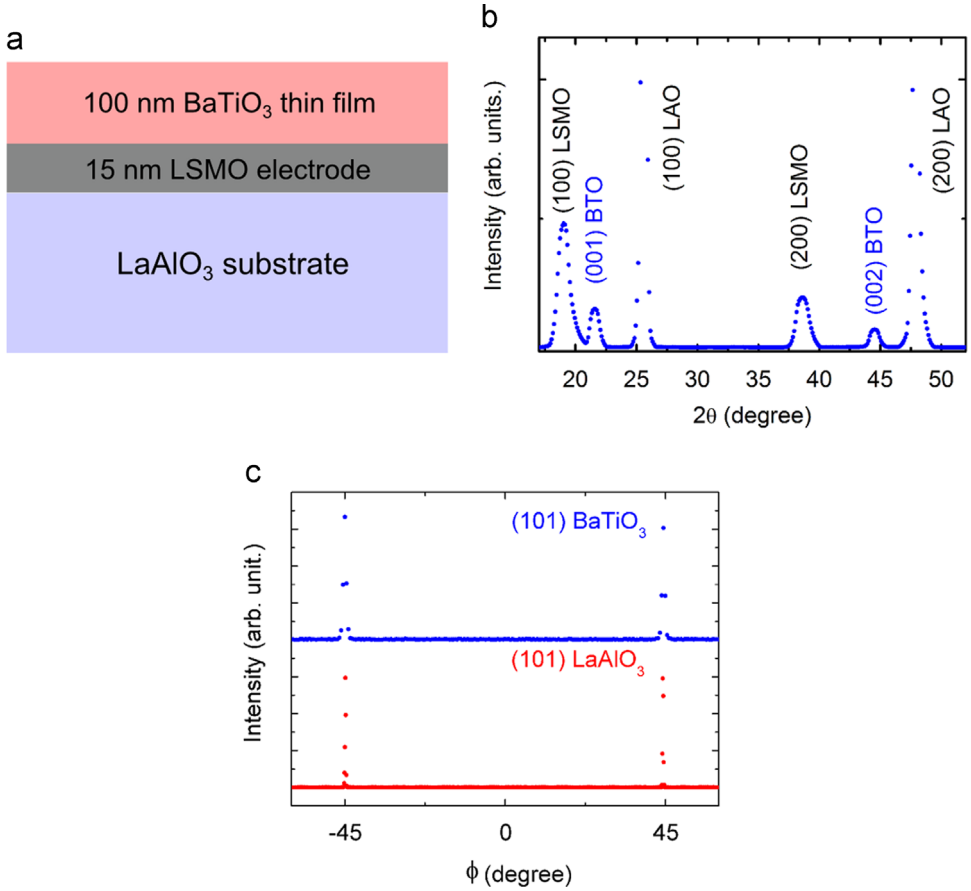

Fig. 1. (a) The schematic drawing of a BTO thin film deposited on LAO substrate with LSMO electrode. (b) The x-ray diffraction pattern of the BTO thin film grown on the LSMO/LAO substrate. (c) The XRD Φ scan for the (101) BTO and (101) LAO peaks.

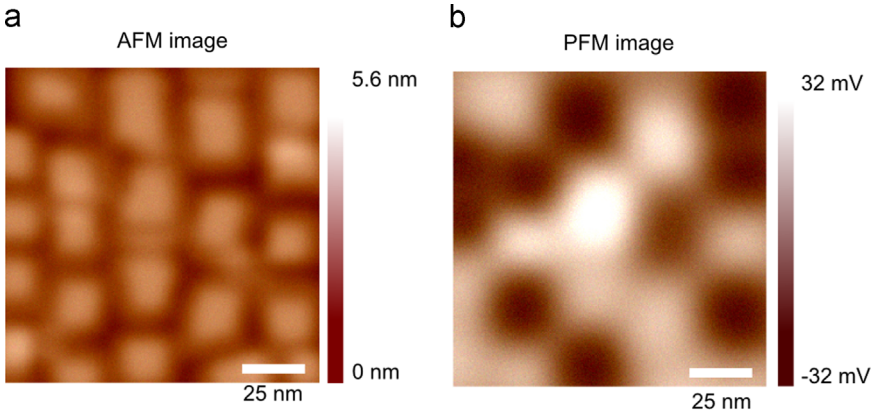

Fig. 2. (a) An AFM image of the BTO thin film shows rectangular-shaped grains. (b) A PFM image of the BTO thin film shows stripe-like mosaic domain structure.

structure of the BTO thin film on LSMO/LAO substrate. The window size is 125 nm and the scale bar is 25 nm. Rectangular-shaped grains were observed on the surface of the BTO thin film as show in Fig. 2(a). From the AFM image, it was inferred that the island growth mode was dominant during the growth of the BTO thin film. The average grain size of the BTO thin film was estimated to be about 25 nm. The root mean square (RMS) surface roughness of the BTO thin film was approximately 6.5 nm. Fig. 2(b) shows the PFM image of the BTO thin film, where stripe-like mosaic domain structure was observed with clear contrast.

To investigate ferroelectric polarization of the epitaxial BTO thin film on LSMO/LAO substrate (BTO1), we considered a nanoscale Pt/BTO/LSMO capacitor made up of the BTO thin film and electrodes. Ferroelectric hysteresis loops were measured at a frequency of 2 kHz as shown in Fig. 3(a). For a comparison, the hysteresis loop of the epitaxial BTO thin film on Pt/MgO substrate (BTO2) reported in our previous work was added [13]. The remnant polarization value of the BTO1 capacitor was 47.3 $\mu C/m^2$, which was significantly higher than the value 33.2 $\mu C/m^2$ of the BTO2 capacitor. As expected, the epitaxial BTO thin films on LSMO/LAO substrates exhibited the enhanced ferroelectric polarization because of the increased tetragonality associated with the strained effect.

In order to evaluate ferroelectric domain wall energy of the epitaxial BTO thin film on LSMO/LAO substrate, we examined domain size of BTO thin films as a function of thickness. By varying the thickness of BTO thin films as 50 nm, 100 nm and 150 nm, ferroelectric domain size vs. thickness curve was plotted on log-log scale in Fig. 3(b). The ferroelectric domain size of the epitaxial BTO thin films closely satisfied the well-known Landau, Lifshitz, and Kittel (LLK) scaling law [17]. According to the LLK scaling law, domain width is proportionally to square root of film thickness as follows:

$$w = Ad^{\gamma}$$

where w is the domain width, A is proportional constant, d is the film thickness, and γ is a scaling exponent (the value close to 1/2). The scaling exponent of the epitaxial BTO thin films fitted by least squares method was estimated to be about 0.56. As shown in Fig. 3 (b), this value was compared with that of $PbTiO_3$ thin films reported previously [18]. Since the scaling exponent is compatible with the domain wall energy [17], it is suggested that the domain wall energy of the epitaxial BTO thin films is higher than that of $PbTiO_3$ thin films, which also imply fine domain structure of the epitaxial BTO thin film.

4. Conclusions

We have grown epitaxial BTO thin films on LAO substrates using LSMO electrodes by PLD. The epitaxial BTO thin films on LSMO/LAO substrates exhibited the increased tetragonallity, compared with the epitaxial BTO thin films on Pt/MgO substrates. This might give rise to higher ferroelectric polarization of the epitaxial BTO thin films on the LSMO/LAO substrates than the epitaxial BTO thin films on Pt/MgO substrates. In a PFM image of the epitaxial BTO thin film on LSMO/LAO substrate, stripe-like mosaic domain structure was observed. From the result of the LLK scaling law, it is inferred that the domain wall energy of the epitaxial BTO thin films on the LSMO/LAO substrates was higher than that of $PbTiO_3$ thin films.

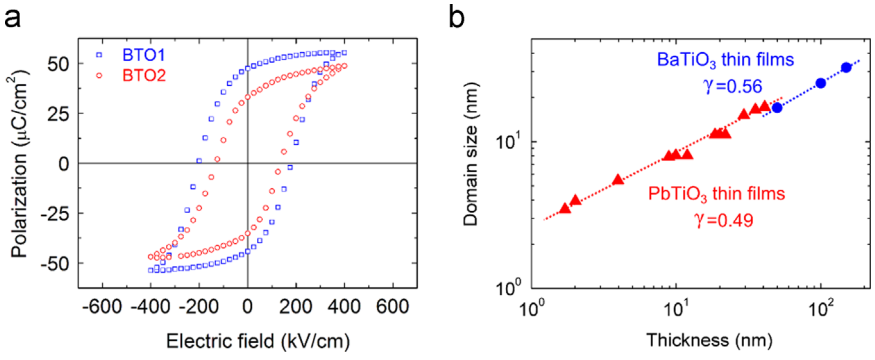

Fig. 3. (a) Ferroelectric hysteresis loops of two BTO thin films on LSMO/LAO (BTO1) and Pt/MgO (BTO2) substrates. (b) The domain size as a function of thickness of the BTO thin films on the LSMO/LAO substrates.

Acknowledgment

This work was supported by the National Research Foundation of Korea (NRF) grants funded by the Korea government (MSIP) (Nos. 2012R1A2A2A01046451 and 2014R1A4A1001690).

References

[1] N. Setter, D. Damjanovic, L. Eng, G. Fox, S. Gevorgian, S. Hong, et al., Ferroelectric thin films: review of materials, properties, and applications, J. Appl. Phys. 100 (2006) 051606–051646.
[2] S.A. Wilson, R.P.J. Jourdain, Q. Zhang, R.A. Dorey, C.R. Bowen, M. Willander, et al., New materials for micro-scale sensors and actuators: an engineering review, Mater. Sci. Eng. R 56 (2007) 1–129.
[3] C.R. Bowen, H.A. Kim, P.M. Weaver, S. Dunn, Piezoelectric and ferroelectric materials and structures for energy harvesting applications, Energy Environ. Sci. 7 (2014) 25–44.
[4] Y. Yuan, Z. Xiao, B. Yang, J. Huang, Arising applications of ferroelectric materials in photovoltaic devices, J. Mater. Chem. A 2 (2014) 6027–6041.
[5] N. Golego, S.A. Studenikin, M. Cocivera, Properties of dielectric $BaTiO_3$ thin films prepared by spray pyrolysis, Chem. Mater. 10 (1998) 2000–2005.
[6] E.-K. Kim, S.-Q. Lee, S.E. Moon, S.-J. Lee, K.-H. Park, Growth and dielectric properties of ferroelectric $BaTiO_3$ thin films for cantilever-type microsensors, Integr. Ferroelectr. 69 (2005) 349–355.
[7] O. Trithaveesak, J. Schubert, C. Buchal, Ferroelectric properties of epitaxial $BaTiO_3$ thin films and heterostructures on different substrates, J. Appl. Phys. 98 (2005) 114101–114107.
[8] J. Li, J. Wang, M. Wuttig, R. Ramesh, N. Wang, B. Ruette, et al., Dramatically enhanced polarization in (001), (101), and (111) $BiFeO_3$ thin films due to epitiaxial-induced transitions, Appl. Phys. Lett. 84 (2004) 5261–5263.
[9] J. Wu, J. Wang, $BiFeO_3$ thin films of (111)-orientation deposited on $SrRuO_3$ buffered $Pt/TiO_2/SiO_2/Si(100)$ substrates, Acta Mater. 58 (2010) 1688–1697.
[10] C.-H. Yang, D. Kan, I. Takeuchi, V. Nagarajan, J. Seidel, Doping $BiFeO_3$: approaches and enhanced functionality, Phys. Chem. Chem. Phys. 14 (2012) 15953–15962.
[11] V.V. Lazenka, M. Lorenz, H. Modarresi, K. Brachwitz, P. Schwinkendorf, T. Böntgen, et al., Effect of rare-earth ion doping on the multiferroic properties of $BiFeO_3$ thin films grown epitaxially on $SrTiO_3$ (100), J. Phys. D: Appl. Phys. 46 (2013) 175006–175009.
[12] N. Kondo, W. Sakamoto, B.-Y. Lee, T. Iijima, J. Kumagai, M. Moriya, et al., Improvement in ferroelectric properties of chemically synthesized lead-free piezoelectric $(K,Na)(Nb,Ta)O_3$ thin films by Mn doping, Jpn. J. Appl. Phys. 49 (2010) (09MA4–6).
[13] Y. Ahn, J. Seo, J. Son, Mn doping effect on the ferroelectric domain structure of $BaTiO_3$ thin films, Electron. Mater. Lett. 11 (2015) 232–235.
[14] A.I. Ali, K. Park, A. Ullah, R. Huh, Y.S. Kim, Ferroelectric enhancement of La-doped $BaTiO_3$ thin films using $SrTiO_3$ buffer layer, Thin Solid Films 551 (2014) 127–130.
[15] K.J. Choi, M. Biegalski, Y.L. Li, A. Sharan, J. Schubert, R. Uecker, et al., Enhancement of ferroelectricity in strained $BaTiO_3$ thin films, Science 306 (2004) 1005–1009.
[16] D.G. Schlom, L.-Q. Chen, C.-B. Eom, K.M. Rabe, S.K. Streiffer, J.-M. Triscone, Strain tuning of ferroelectric thin films, Annu. Rev. Mater. Res. 37 (2007) 589–626.
[17] G. Catalan, H. Béa, S. Fusil, M. Bibes, P. Paruch, A. Barthélémy, et al., Fractal dimension and size scaling of domains in thin films of multiferroic $BiFeO_3$, Phys. Rev. Lett. 100 (2008) 027602–027604.
[18] W.-H. Kim, J. Son, Triangular ferroelectric domains of highly (111)-oriented $NaNbO_3$ thin film on a glass substrate, Electron. Mater. Lett. 10 (2014) 107–110.